FISEVIER

Contents lists available at ScienceDirect

Journal of Building Engineering

journal homepage: www.elsevier.com/locate/jobe



A multi-stage analysis of air leakage and acoustic performance on a full-scale test chamber

A. Elsaei ^{a,c}, M. Machimbarrena ^{b,d,*}, A. Meiss ^{a,d}, I. Poza-Casado ^{a,d}, M.A. Padilla-Marcos ^{a,d}

ARTICLE INFO

Keywords: Air infiltration Airtightness Sound transmission Flow regimes Airborne sound insulation

ABSTRACT

It is imperative to comprehend the intricate relationship between air infiltration and sound transmission in building systems to optimise energy efficiency and acoustic comfort. This study focuses on measuring the performance of a separating wall between two spaces in terms of sound insulation and airtightness, under different air flow path configurations.

Airtightness and sound insulation measurements were made on a test sample wall mounted in an accredited sound insulation facility, while subsequently increasing the number and size of artificially drilled openings. The diameter of these apertures ranged from 0.67 to 7.09 cm, with the total area of the apertures varying up to 39.50 cm². The variation in diameter and the total number of apertures had a dual impact: it affected airtightness and the flow regime and energy dissipation within the apertures, which in turn may affect sound insulation.

The acoustic results presented an unexpected behaviour: conventional wisdom suggests that increasing the number of openings should lead to a decrease in sound insulation; however, the study observed that adding relatively small holes $(0.67/1.4~\rm cm$ diameter) resulted in constant or less sound transmission. The results suggest that the diameter of holes affects the flow regime, as indicated by the n exponent values that characterize flow behavior. Furthermore, these variations influence energy dissipation within the openings, which in turn may impact sound insulation. This observation underscores the intricate interplay between airflow and sound transmission in building systems. Further research is required so that the acoustic firm of cracks can be used to estimate the size of cracks in buildings and to provide a prioritization criterion when undertaking retrofitting.

1. Introduction

Improving building quality involves multiple dimensions, one of which is enhancing occupant comfort, encompassing factors such as indoor air quality, acoustic performance, lighting, and hydrothermal regulation. Among these factors, building air leakages through cracks significantly impact acoustic, hydrothermal, and air quality performance. These cracks facilitate unintended air exchange,

a Dpto. Construcciones Arquitectónicas I.T. y M.M.C.T.E, E.T.S. de Arquitectura, Universidad de Valladolid, Spain

^b Dpto. Física Aplicada, Universidad de Valladolid, Spain

^c Architecture, Built Environment and Construction Engineering Department (ABC), Politecnico di Milano, Italy

^d GIR Arquitectura y Energía, Universidad de Valladolid, Spain

^{*} Corresponding author. Dpto. Física Aplicada, Universidad de Valladolid, Spain. *E-mail address:* maria.machimbarrena@uva.es (M. Machimbarrena).

thereby serving as pathways for sound transmission and affecting acoustic comfort.

Although these issues are usually examined independently, there is an increasing acknowledgement of the interconnected nature of air infiltration and sound transmission loss within buildings. Investigating the interplay between these factors is necessary, as better characterisation and measurement techniques could enhance construction efficiency, reduce project timelines, and lower the corresponding costs. This is especially crucial in retrofits, where enhancing airtightness and the sound insulation of the façade is a priority.

Despite the apparent connections between air infiltration and sound transmission loss, research that seeks to establish a correlation between the two phenomena is under development. Some researchers have focused in the past on how to establish a mathematical relationship between sound insulation and air infiltration [1–6], while others have focused on locating or estimating air infiltration based on different acoustic methods [7–14]. In numerous studies, the prospective impact of variables such as crack size, shape, position and material, in addition to other influencing factors, on both sound insulation and airflow has been examined in diverse methodologies [3,15–20].

One of the earliest attempts to calculate the effect of an opening in a wall on its sound attenuation was made by Ref. [15,16], who noted that the sound insulation decreased with increasing size of the opening and also as the opening deviated from the centre to the edges/corners of the wall. Subsequent research by Ref. [3] studied the relationship between airflow and sound attenuation for various-width slits, highlighting that a simple relation between sound attenuation and straight-slits' width (and consequently airflow) is only valid for relatively wide slits.

The intricate interplay between sound propagation and air infiltration behaviour through cracks was further investigated by Ref. [20], who performed a series of sound pressure level measurements across diverse slit configurations. Their study tested slits of different widths (ranging from 0.5 to 2.0 mm) and designs, including straight slits, slits with bends, and slits covered with foil or coupled to damped cavities. The results of this study revealed substantial variations in sound transmission based on the geometric and material properties of the slits. It was also observed that for slits covered with lightweight foil, there was a decrease in airflow while the sound transmission remained constant or even increased, likely due to a more precise impedance match between the room and the slits. In a theoretical and experimental study [3], studied the sound transmission loss (STL) through slits of varying sizes (width ranging from 1 to 10 mm; depth from 50 to 152 mm). Their findings indicated that the resonant frequencies of the slit STL are strongly related to the size of the openings, particularly for relatively wide openings. In this case, the resonant frequencies could be used to estimate airflow. On the other hand, it was also observed that in the case of smaller size openings, the viscous effects increased with increasing values of the ratio depth/width and should be the focus of further study when considering the use of STL to estimate air leakage.

Similarly [21], investigated the correlation between STL and air leakage across cracks with different shapes, sizes, and materials using controlled laboratory experiments and field testing. The study tested circular holes ranging from 1 to 25 mm in diameter, rectangular slits with lengths between 1 and 10 cm and widths ranging from 1 to 5 mm. Additionally, irregular and complex crack geometries were designed to simulate realistic building leakage paths. Based on these laboratory tests, an empirical relationship between STL and air leakage was developed. However, it was observed that when this relationship was applied in field conditions, STL measurements often underestimated airtightness compared to blower door tests, particularly for complex crack geometries.

In another study [17], proposed a high-frequency impulse response technique to estimate leakage sizes. The sound reduction index was measured on two different walls (plywood and acrylic) in their original state and with different opening diameters (4, 6, 8, and 10 mm). The findings, as anticipated, revealed that the sound reduction index decreased with increasing hole size, thereby suggesting a correlation between the two variables. However, a direct relationship between hole size and sound reduction index at specific frequencies could not be established.

A recent study on this subject was conducted by Ref. [18]. Although the research focuses on outdoor air intakes or vents, which often have a silencer mounted inside or an end reflector, preliminary tests were conducted on fully open vents. The findings revealed that, for openings with diameters varying from 6 to 12 mm, the sound insulation was affected only at high frequencies and thus the single number quantities were very little affected, whereas, as the opening diameter increased, the frequency at where the effect was visible decreased. In this case study, the openings were tested in three different positions and no significant difference was observed except at one specific frequency (125 Hz) and one single position, results which were not conclusive concerning the potential effect of opening position. In summary, for small circular openings, the aperture location (centre, edge, or corner) did not significantly influence single-number sound insulation values. In contrast, earlier research [15,16] involving larger openings (circular openings 2–30 mm in diameter and slit-shaped openings 0.1 and 1.1 cm in width) demonstrated that centrally located openings in a wall provided better sound insulation compared to those positioned near edges or corners, due to sound pressure increase in these regions. This highlights that, for relatively small openings, the spatial placement within the wall has a negligible impact on sound insulation.

[22] studied whether different leak sizes could be reliably estimated using acoustic measurement techniques. Measurements were made in a scale model setup where several wall and slit configurations were tested. They found that while the acoustic method uncertainty remains significant (± 50 %), order-of-magnitude estimates of single leak sizes through observed linear correlational trends can be achieved.

This research focuses on further studying the effect of opening size and spatial distribution of wall openings on sound insulation, using a staged experimental setup within a controlled environment. By varying the size and arrangement of manually drilled openings in a structured experimental setup, the study examines the interplay between airtightness and sound transmission across different openings' configurations. The research specifically addresses two central questions: (1) To what extent do variations in the size, relative position and configuration of openings influence airflow and thus acoustic energy dissipation? (2) How is sound insulation performance related to airflow characteristics in the tested samples? The findings aim to provide further insight concerning the correlation between airtightness and sound insulation, since this approach represents a promising step toward quantifying air leaks using acoustic methods, offering a potentially powerful tool for building retrofitting by saving both time and cost.

2. Methodology

A sample wall has been mounted in an accredited airborne sound insulation laboratory, separating two acoustically independent and airtight rooms: one is considered the receiving room (Room 1) and the other is the source room (Room 2). The schematic layout of the setup is depicted in Fig. 1a, and a 3D model of the measurement setup is shown in Fig. 1b.

Fig. 2a and b show the actual receiving and source rooms, respectively. Additionally, Fig. 2c provides an external view of the two test rooms, highlighting their structure. The wall width is 360 cm and the height is 280 cm. It is composed of large-format hollow bricks, plastered with a 1.5 cm cement layer on one side and a 0.5 cm cement layer on the other, with a total wall thickness of 22 cm. The bricks are joined together using tongue-and-groove joints, with a cementitious mortar adhesive applied between rows. The perimeter of the sample wall is sealed with cement mortar along the sides and bottom, while the upper edge is sealed with gypsum plaster, as shown in Fig. 2d.

This experimental setup aims to investigate the interplay between airtightness, airflow regimes, and sound insulation.

2.1. Measurement concept and laboratory equipment

Sound insulation measurements were conducted at AUDIOTEC's accredited airborne sound insulation laboratory, following ISO 10140-2 [23], an omnidirectional sound source was placed in the source room, Room 2, in two different positions and the average sound pressure levels in both the source and the receiving room was measured using rotating microphone boom typical for laboratory building acoustics tests. Three sets of measurements for each source position have been made. Measurements have always been done by the same laboratory accredited personnel, equipment and setup, which is under repeatability conditions.

The sound reduction index R was then calculated in third-octave bands according to Equation (1):

$$R = L_1 - L_2 + 10 \lg (S/A)$$
 (Eq.1)

where L_1 and L_2 represent the average sound pressure level [dB] in the source and receiving rooms, respectively, S is the area of the free test opening in which the sample wall is installed [m^2], and A is the equivalent sound absorption area in the receiving room [m^2].

The corresponding standardized sound insulation descriptors, R_w , C, and C_{tr} , were also calculated according to ISO 717-1 [24]. For this study, the descriptor $R_{A,tr} \approx R_w + C_{tr}$ has been chosen due to its use in façade sound insulation characterization. (R_w : Weighted sound reduction index [dB], C_{tr} : Spectrum Adaptation Term for Pink Noise [dB], C_{tr} : Spectrum Adaptation Term for Traffic Noise [dB], $R_{A,tr}$: Traffic Noise Weighted Sound Reduction Index [dB]). According to ISO 12999-1 [25], in these circumstances, the standard uncertainty for $R_{A,tr}$ is 0.7 dB.

The airtightness tests were conducted using the fan pressurization method following ISO 9972 [26]. This method is also known as Blower Door test and it is the most common approach for evaluating envelope airtightness and is recognized in both national and international standards. [27]. The equipment used was the Blower Door MiniFan (5 m^3/h - 2300 m^3/h) along with a pressure sensor. Calibration according to manufacturer specifications was ensured.

In this procedure, a controlled pressure differential was generated by positioning a fan at the door opening of the receiving room while leaving the door open in the source room. Each airtightness test involves a series of automatic measurements conducted under a controlled depressurization process with pressure differentials ranging from 4 Pa to 80 Pa. This technique is based on the power law equation, which is used to represent the relationship between the pressure difference and air flow rate for different crack and opening geometries, also described as the air permeability law (Equation (2)) [28]:

$$q = C \cdot \Delta p^n$$
 (Eq.2)

where q is the measured air flow [m³/h] at a reference pressure difference, Δp is the pressure difference between both sides of the envelope [Pa], C is the air leakage coefficient [m³/(h·Paⁿ)], and n exponent.

The n exponent characterizes the airflow behaviour through the building envelope and describes the influence of major component

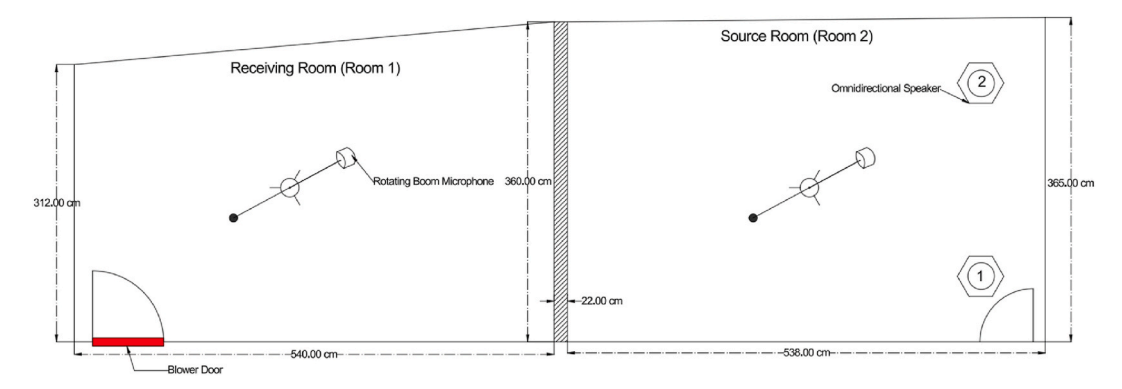


Fig. 1a. Schematic drawing of the test rooms and measurement setup.

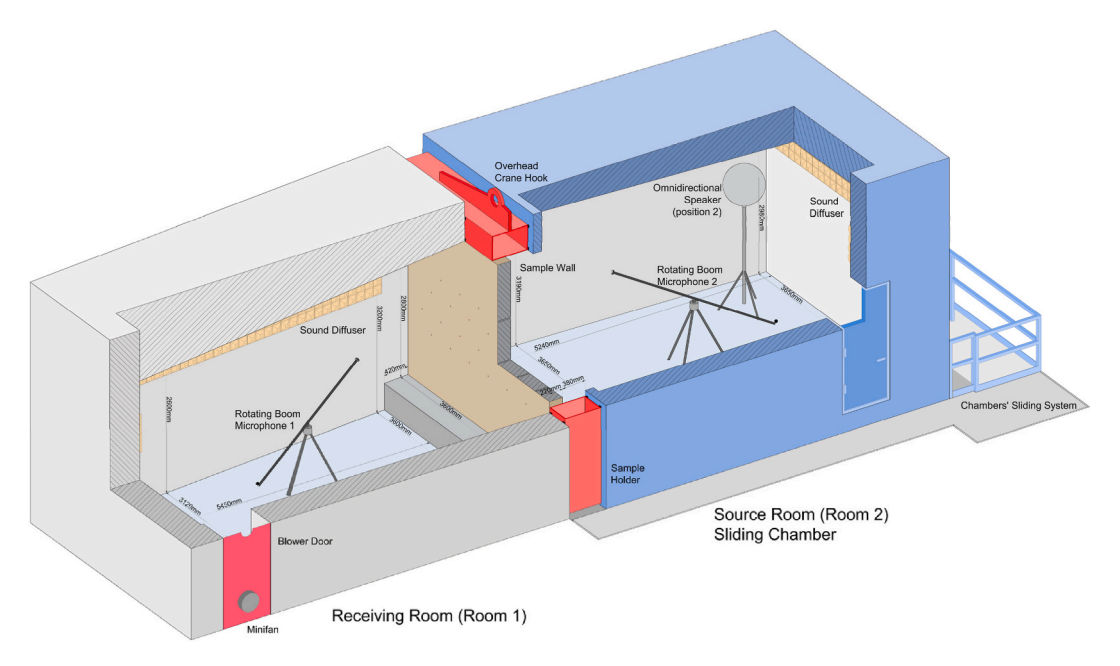


Fig. 1b. 3D model of laboratory facilities and measurement setup.



 $\textbf{Fig. 2a.} \ \ \text{Receiving room (Room 1)}.$



Fig. 2b. Source room (Room 2).

leakages and background leakage across the envelope, providing insight into the relative size and nature of the most significant leaks. Typical values for n range between 0.5 and 1. Values of n near 0.5 are generally associated with large openings and short airflow paths, with nozzles serving as a typical example; these values are difficult to obtain in building tests and are typical of laboratory tests. An n



Fig. 2c. Room 1 (grey)/room 2 (blue).



Fig. 2d. Sample wall in original stage (Stage 0).

exponent greater than 0.55 is indicative of large and significant cracks in the walls, with a dominantly turbulent airflow pattern. When this value increases, turbulence in the flow decreases until a transition regime to laminar flow around n equal to 0.65 is reached; in such cases, the openings are characterised by small joints and narrow cracks (a mixed laminar-turbulent pattern), which are typical of window frames and façade junctions [29,30].

By using the Blower Door device Δp and q are measured simultaneously. After that, by plotting both parameters, C and n can be calculated from the graph. Results are expressed as the air flow at a reference pressure of 50 Pa, q_{50} [m³/h]. The estimated error obtained for q_{50} remains between ± 0.2 and ± 1.0 %, and between ± 0.003 and ± 0.014 for the flow coefficient exponent, n.

2.2. Stepwise modifications and sequential measurements of the wall sample

This section describes in detail the different scenarios that have been created for this investigation. Each stage was designed to progressively evaluate the impact of specific parameters on air leakage and sound insulation. For each configuration, tests were performed once, although some were repeated as control tests during stage 1. To improve repeatability, the same operators completed the whole measurement campaign using the same equipment and method in the mentioned rooms. The relationship between the stages and the rationale for each modification is discussed below.

Stage 0: Reference Stage (baseline)

The initial airtightness and sound insulation measurements were performed on the wall sample in its original, undrilled state (Table 1, Fig. 2d). Therefore, the Opening Area (OA) is 0 at this stage. This stage served as the reference for all subsequent modifications.

Stage 1: Openings configuration - drilling of 1.40 cm diameter holes

The purpose of this first set of measurements was to evaluate how increasing the OA [cm²] progressively influences sound

Table 1Stage 0 - Summary of measurement scenario and wall modifications.

STAGE 0:				
Strategy	Description	N° holes open	Diameter, Φ [cm]	OA [cm ²]
Wall in original state	Fig. 2d Used as the baseline.	0	0.00	0.00

attenuation and to assess airtightness variations. Therefore, sequential and systematic modifications were made to the wall. A total of 24 holes were drilled into the wall, following a predetermined layout as shown in Table 2, Fig. 3a and b. A detailed drawing of the sample wall showing its dimensions and the hole distribution over the wall illustrated in Fig. 4. Due to the characteristics of the wall and the inherent challenges of the drilling process, achieving perfectly uniform hole dimensions was not feasible. Taking this variability into account, the average hole diameter resulted 1.40 cm (corresponding to an opening area, $OA = 1.54 \text{ cm}^2$). This introduces an additional source of uncertainty to the experimental results, particularly in the interpretation of the airflow and sound attenuation measurements. After drilling four holes, airtightness and sound insulation were measured. A total of 7 airtightness and sound insulation measurements tests were performed. By the end of this stage, with 24 drilled holes, the total opening area reached $OA = 36.96 \text{ cm}^2$.

Stage 2: Opening configuration - controlled opening of 0.67 cm diameter tabs

To address variability in the drilled holes, all holes were covered with control tabs featuring a standardized diameter of 0.67 cm, as shown in Fig. 5a, corresponding to an opening area of OA = 0.35 cm 2 . The tabs' perimeter was sealed using custom putty made from high-durability polyurethane (density 1.26 kg/l). This step ensured consistent airflow and sound transmission measurements. The wall with the configuration of the tabs is shown in Table 3 and Fig. 5b. These tabs allowed for precise control over the equivalent opening size and enabled the design of different opening configurations. These configurations were designed to investigate the impact of opening size, opening location and total opening area on airborne sound insulation and airflow dynamics, with a particular focus on the frictional and viscous effects associated with smaller diameters. This opening area standardization minimized uncertainty related to opening dimensions and facilitated consistent experimental comparisons.

• Phase 1: sequential opening of tabs: Initially, the airtightness and acoustic results for the fully closed tabs scenario were compared to the measurements from Stage 0 (Reference Stage) to verify the integrity of the tab configuration. A smoke generator was used from Room 2 while depressurizing Room 1 with the blower door system to check the effectiveness of the tabs and to ensure the wall was airtight after mounting the tabs. This step confirmed the reliability of the tab installation, ensuring the results were accurate for further analysis.

Then, the plastic tabs were incrementally opened following the same sequence as in Stage 1, as illustrated in Fig. 3b, and airtightness and sound insulation measurements were taken after opening every set of 4 holes. Tests were conducted for the wall in its fully sealed state, as well as after 4, 8, 12, 16, 20, and all 24 holes were opened (resulting in a final total opening area, $OA = 8.46 \text{ cm}^2$). Consequently, this phase involved 7 airtightness and 7 acoustic tests. It is worth mentioning that in all cases, the airtightness tests were performed under depressurization conditions, where air is pulled out of the room. This ensures consistency of the experimental setup, as depressurization tends to close the tabs, minimizing additional leakage.

In the next two phases, additional measurements were made using a different strategy. The holes were grouped in different ways, depending on the specific purpose of the set of measurements, as it is explained hereinafter.

• Phase 2: sequential opening of patterns (4 tabs for each pattern):

The purpose of this phase was to further investigate how the spatial distribution and relative positioning of the small tabs' openings affected sound transmission characteristics. In this phase, sound insulation measurements have been done while the tabs were opened in groups of four following a specific pattern, as illustrated in Fig. 5c, resulting in a total of six sets of measurements. Airtightness assessment was conducted while opening the tabs according to the same specific patterns without closing the previously opened tabs. In this case, the opening order is different than in phase 1. The airtightness results are thus used to confirm the airflow consistency for all phases in this stage. The acoustic results from this phase were intended to be compared with those from **Phase 1** and **Phase 3**, which involve different opening areas and configurations, to provide a comprehensive understanding of how the opening arrangement impacts the acoustic performance of the wall.

Table 2Stage 1 - Summary of measurement scenario and wall modifications.

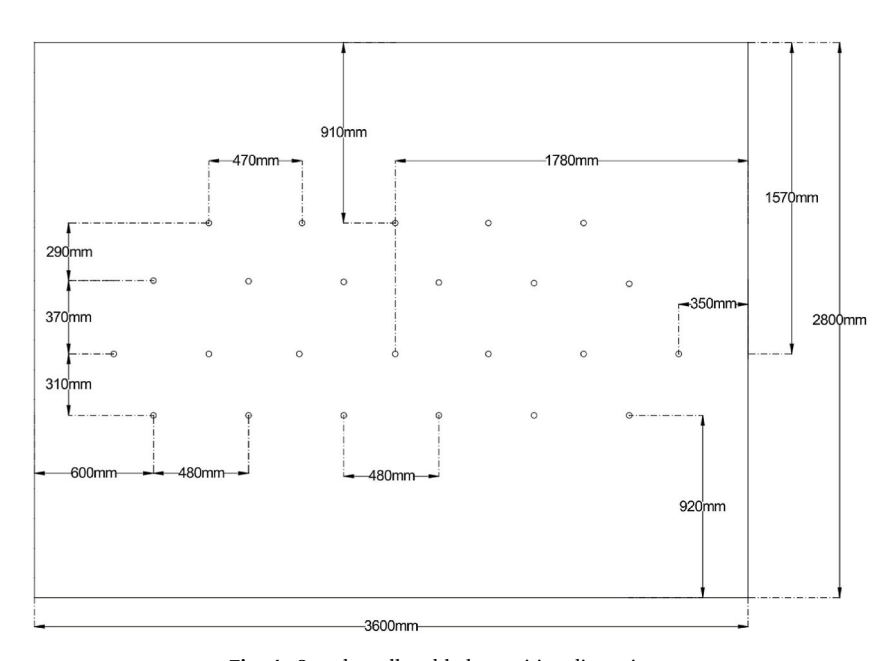
STAGE 1: Drilling of small holes								
Strategy	Description	N° holes open	Diameter, Φ [cm]	OA [cm ²]				
Drilling 24 holes according to sequence shown in Fig. 3b.	Fig. 3a	4	1.40	6.16				
		8		12.32				
		12		18.48				
		16		24.64				
		20		30.81				
		24		36.96				



Fig. 3a. Stage 1: The 24 drilled small holes ($\Phi = 1.4$ cm).

		24		22		20		21		23		
	ຳ9		°17		15		°14		ำ6		ใ8	
7		3		3		٩		2		°4		6
	12		។1		9		8		90		ำ3	

Fig. 3b. Sequence of drilling holes in Stage 1 and opening tabs in Stage 2.



 $\textbf{Fig. 4.} \ \ \textbf{Sample wall and holes position dimensions.}$

• Phase 3: Horizontal and vertical patterns: Building on the insights gained from Phases 1 and 2, this phase aimed to explore the effect of opening alignment by arranging the holes in both horizontal and vertical patterns, as shown in Fig. 5d and e. Five patterns were formed, resulting in five sets of measurements for both airtightness and sound insulation.

This phase sought to determine whether the orientation of the holes relative to the wall geometry had a significant impact on sound transmission. In this phase, the number of openings in each row varied, resulting in different total OA for each pattern. This variation in OA allowed for a broader analysis of the relationship between the opening area and both sound insulation and airtightness characteristics.

Stage 3: Single opening configuration.



Fig. 5a. *Stage 2*: The controlled plastic tabs ($\Phi = 0.67$ cm).

Table 3
Stage 2 - Summary of measurement scenario and wall modifications.

STAGE 2: Contro	lled opening of plastic tabs s	shown in Fig. 2 d			
Strategy	Description		N° holes open	Diameter, Φ [cm]	OA [cm ²]
Phase 1	Fig. 5b		0 0.67	0.67	0
			4		1.41
			8		2.82
			12		4.23
			16		5.64
			20		7.05
			24		8.46
Phase 2	Fig. 5c	Pattern 1	4	0.67	1.41
		Pattern 2	4		1.41
		Pattern 3	4		1.41
		Pattern 4	4		1.41
		Pattern 5	4		1.41
		Pattern 6	4		1.41
Phase 3	Fig. 5d	H1	11	0.67	3.88
		H2	13		4.59
		H3	13		4.59
	Fig. 5e	V1 & V2	16		5.64
	Fig. 5e	V1	8		2.82
	-	Vertical 2	8		2.82



Fig. 5b. Stage 2: The 24 controlled openings of smaller holes.

This experimental stage investigated how a large, centralized opening behaves compared to a group of smaller openings with equivalent total OA (Table 4). This could help understand how a larger air pathway would affect the flow regime and sound insulation and provide additional data to further investigate the effects of opening size on airflow and sound transmission. As a first step, all tabs were closed on the source side (Room 2), and the previously drilled small holes were sealed on the receiving room side (Room 1), restoring the wall to its original state as in Stage 0. Then a single large circular hole was drilled in the middle of the wall, as shown in Fig. 6a, and a 7.09 cm diameter tube was inserted and sealed into this hole. The opening area in this case was equivalent to 112 small tabs opened.

In addition to the first inserted tube, five smaller tubes with varying diameters (5.69, 4.64, 3.28, 2.68, and 1.89 cm) were designed to have opening areas equivalent to 72, 48, 24, 16, and 8 small tabs, respectively. These tubes were 3D-printed using UV-LED resin, as shown in Fig. 6b. Resin printing enables micrometer-level precision, which reduces the error when calculating the corresponding

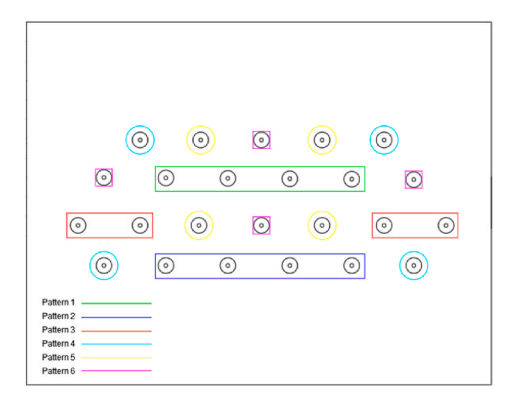


Fig. 5c. Stage 2- Phase 2: 4 hole tab patterns (Patterns 1 to 6).

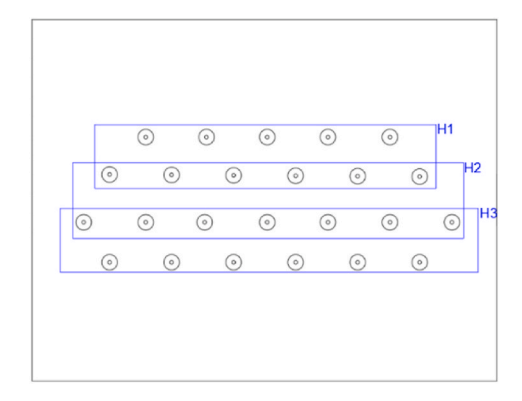


Fig. 5d. Stage 2- Phase 3: Horizontal patterns (H1 to H3).

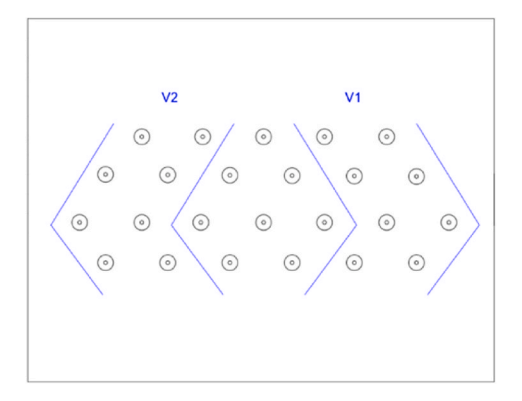


Fig. 5e. Stage 2- Phase 3: Vertical patterns (V1 and V2).

Table 4Stage 3 - Summary of measurement scenario and wall modifications.

STAGE 3: Larger resin tubes openings							
Strategy	Description	N° holes open	Diameter, Φ [cm]	OA [cm ²]			
Sequential resin tube configurations	Fig. 6a, b, 6c	1	7.09	39.50			
			5.69	25.39			
			4.64	16.92			
			3.28	8.46			
			2.68	5.64			
			1.89	2.82			



Fig. 6a. Stage 3: Large opening location in the middle of the wall. Small tabs closed.

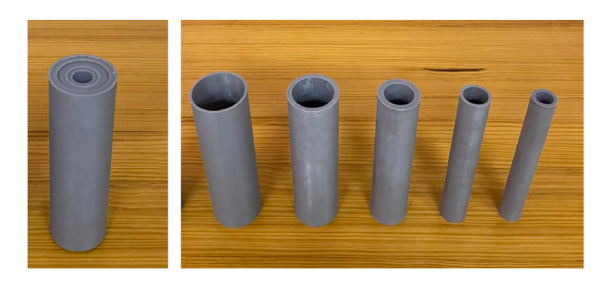


Fig. 6b. Stage 3: 3D-printed resin tubes with diameters from 1.89 to 5.9 cm.

opening area. These tubes were sequentially inserted into the 7.09 cm diameter opening for airtightness and sound insulation tests, as shown in Fig. 6c. The airtightness tests were conducted solely to verify that experimental conditions remained consistent with previous stages, ensuring the validity of subsequent acoustic measurements. In total, 6 sets of airtightness and sound insulation tests were conducted in this stage, considering a total OA coincident with some of the measurements performed at Stage 1. This approach allowed us to compare the behavior of a group of small, distributed openings with that of a single, large, centralized opening of equivalent total OA and to determine if the size and relative position of the opening significantly influenced the acoustic performance.

The results of these tests will be presented and analyzed in the following sections, providing a deeper understanding of the interplay between airtightness and acoustic performance.

3. Results

3.1. Airtightness measurements results

The results of the Blower Door test (Fig. 7) show a clear correlation between the opening area (OA) and the air leakage rate (q_{50}) at a reference pressure of 50 Pa and for all the different opening conditions under study, as it was expected. Furthermore, comparing the air leakage rates under "completely sealed conditions" in Stage 0, and with all tabs closed in Stage 2, reveals almost similar q_{50} values, approximately 175 m³/h for Stage 0 and 181 m³/h for Stage 2. This minor difference, corresponding to approximately 3.4 % of the total airflow, highlights the effectiveness of the plastic tabs in maintaining airtightness and allows for tests with the tabs closed,



Fig. 6c. Stage 3: Large openings. Detail.

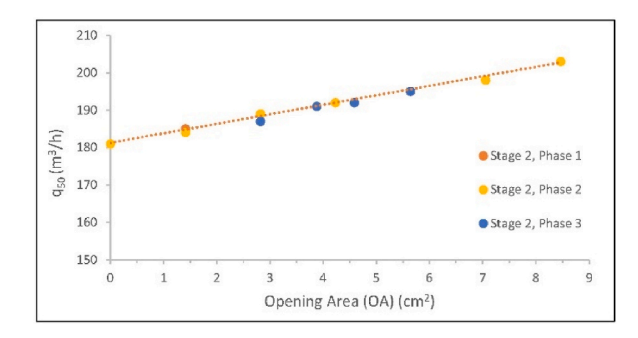


Fig. 7. Air pressurization test results focus on Stage 2.

effectively simulating conditions without any drilling. The reliability of the results is further ensured by the very small, standardised error margins of the tests, which were carried out under laboratory conditions: q_{50} (min. \pm 0.2 %; max.1.0 %); n exponent (min. \pm 0.003; max. \pm 0.014).

3.2. Leakage configuration and acoustic performance

The results for the sound insulation measurements for different configurations of the opening area (OA) for Stages 1, 2 and 3 are shown in Fig. 8a. The correlation between $R_{A,tr}$ and OA was statistically analyzed by addressing normality and linearity to apply Pearson's or Spearman's correlation coefficients. Statistical significance was assessed at the 0.05 level.

For stage 1, variations within a narrow range of approximately 1 dB are observed in $R_{A,tr}$. Even as the number of holes increases, all acoustic descriptors remain largely unchanged. In this regard, for Stage 1, even though the range of $R_{A,tr}$ values are acoustically negligible, a strong correlation was observed between OA and $R_{A,tr}$ (r = 0.969, p = 0.031). Contrary to what would be expected, the correlation is positive, with $R_{A,tr}$ showing a slight tendency to increase as OA grows.

For stage 2, again $R_{A,tr}$ values remained nearly constant, yielding a weak positive correlation and a non-significant Spearman's coefficient (r = 0.456, p = 0.057). These findings indicate that the relationship in Stage 2 is not robust due to the restricted variability of $R_{A,tr}$.

On the other hand, the results for Stage 3 show a noticeable decrease in the sound insulation parameter, $R_{A,tr}$, as the opening area of the central hole increases. A very strong and significant negative association (r = -0.997, p = 0.004) was found.

Fig. 8b represents in detail the results for the three different phases in Stage 2. In this case, it is clear that altering the opening location, whether near the centre of the wall or distributed further apart, while changing the opening patterns, has minimal impact on the sound insulation performance, as indicated by the consistent $R_{A,r}$ values. Similarly, increasing the total opening area by adding more open tabs does not result in changes in sound insulation performance.

Given the limitations of focusing solely on single quantities like $R_{A,tr}$ or R_w —which are calculated based on specific frequency ranges— a detailed analysis of the sound reduction index levels across the typical building acoustics frequency range is shown in Fig. 9a for Stage 2 and in Fig. 9b for Stage 3. The spectral representation shows no anomalous results at any specific third octave band as more tabs are opened in Stage 2. In Stage 3, there is a decrease in the sound insulation above 500 Hz as the opening diameter increases, since larger openings may propagate acoustic modes more efficiently. Besides, a strong mechanical resonance is observed at approximately a fundamental frequency of 630 Hz and its first harmonic 1250 Hz. This resonant effect is better observed for the larger diameter resin tubes, where the airflow resistance is lower, producing less interaction and damping within the tube and where the surface area-to-volume ratio is also smaller, allowing for stronger resonances.

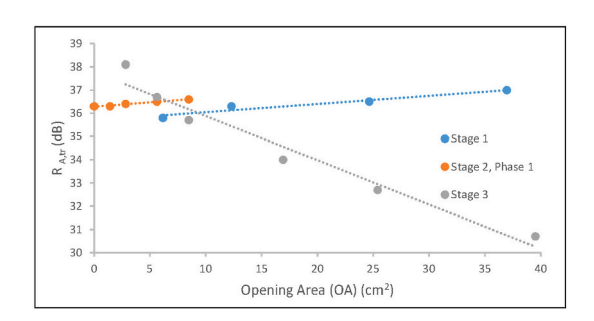


Fig. 8a. Sound insulation $(R_{A,tr})$ variation with the opening area (OA) for stages 1, 2, and 3.

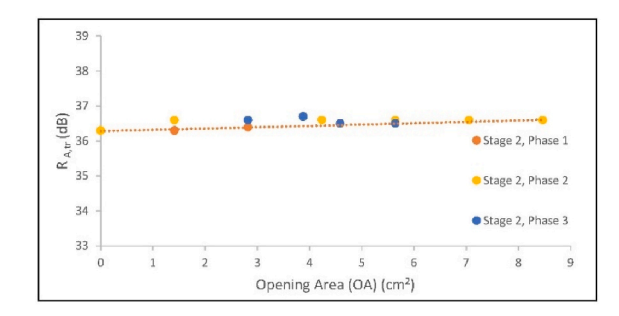


Fig. 8b. Sound Insulation $(R_{A,tr})$ Variation with the Opening Area (OA); focus on Stage 2.

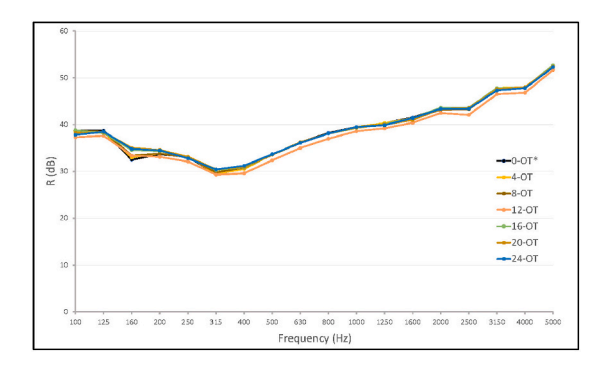


Fig. 9a. Sound Reduction Index, in third-octave bands. Stage 2 - Phase 1 (N°-OT: Open Tabs).

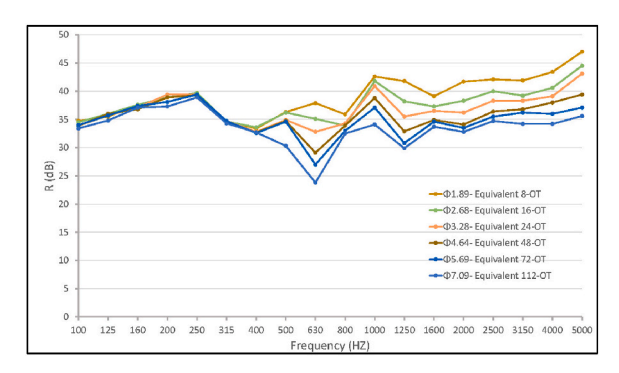


Fig. 9b. Sound Reduction Index, in third-octave bands. Stage 3 (ΦTube- Equivalent OT: Open Tabs).

Table 5 A variation of the Exponent n of the air permeability law with ISA for Stages 2 and 3.

		Stage 2-Phase 1 (tabs)			Stage 3 (tubes)			
N° OT ^a	OA (cm ²)	ISA (cm ²)	R _{A,tr} (dB)	n	Φ (cm)	ISA (cm ²)	R _{A,tr} (dB)	n
0	0.00	0.00	36.3	0.646				
4	1.41	218.90	36.3	0.648				
8	2.82	437.81	36.4	0.640	1.89	154.38	38.1	0.634
16	5.64	875.62	36.5	0.636	2.68	218.91	36.7	0.617
24	8.46	1313.43	36.6	0.629	3.28	267.92	35.7	0.617
48	16.93				4.64	379.00	34.0	0.607
72	25.39				5.69	464.77	32.7	0.604
112	39.50				7.09	579.12	30.7	0.588

 $^{^{\}rm a}\,$ No. of Open Tabs (OT) for Stage 2/Equivalent number of Open Tabs for Stage 3.

4. Discussion

Airtightness results are consistent with expectations (airflow increase with opening area increase) and are used as a point of reference for comparing the subsequent acoustic measurements. The findings from the acoustic measurements appear paradoxical at first: an increase in the opening area does not necessarily correspond to a decrease in the sound insulation level (Stages 1 and 2). The possible explanation for these tests under controlled laboratory conditions must basically consider the magnitude of the contact area between the air and the interior tube surface (Internal Surface Area, ISA), as well as the flow regime adopted by the air in the infiltration path (Table 5).

In Stage 2 (Fig. 10a and b), the variation of the sound reduction index $R_{A,rr}$ is negligible despite the opening of more tabs (with the corresponding increase in the ISA), as shown in Fig. 9a. The analysis revealed a positive correlation between $R_{A,rr}$ and ISA (r = 0.987, p = 0.002). The tabs have a sufficiently small diameter (more friction area or flow surface area inside the full path), as verified by the practically constant value of the n exponent (0.629–0.648) This means that the turbulent flow dissipates more sound energy in its path, and thus transmits less sound pressure levels to the other side, just as it would in the typical cracks present in the building.

With regard to the position of openings within the wall, this was studied through the three different phases in Stage 2. The spatial placement of openings demonstrated minimal impact on sound insulation performance for the small opening sizes tested in this study (6.7 mm diameter). These results align with those by Nurzyński [18] who found that, for relatively small openings, the spatial placement within the wall has minimal impact on the sound insulation.

In Stage 3 (Fig. 10a and b), the variation in the $R_{A,r}$ becomes more evident with a negative correlation between $R_{A,r}$ and ISA (r = -0.998, p = 0.000). The smallest diameter that was tested (1.89 cm) is almost three times the diameter of the plastic tabs (0.67 cm) of Stage 2, and this progression is in line with the increase in the opening area. The larger diameter causes the flow to acquire the characteristics of a nozzle, where a significant portion of the flow passing through the opening does not dissipate its sound energy upon contact with the ISA. The aerodynamic conditions of this situation are verified through the evolution of the n exponent (0.639-0.588), which moves towards significant cracks, typical of intentional holes in buildings rather than pathologies within them.

5. Conclusions

This study investigates the interplay between air leakage, sound transmission and flow regimes through different diameters of holes that have been intentionally perforated through a sample wall mounted between two rooms in an accredited airborne sound insulation laboratory. The acoustic behaviour observed was influenced not only by the size of the opening area, but also by the conjunction between the ISA and the n exponent.

It has been demonstrated that smaller apertures, such as the typical cracks and air leakages that are present in the walls of buildings, produce unique acoustic behaviours. These are partially attributed to frictional and viscous effects, which dissipate sound energy more effectively than larger apertures with the same opening area. This behaviour was reflected in the values of the n exponent, which indicated the characteristics of the air penetration openings, which are manifested in the flow regime of the air that passes through them. In contrast, with larger-diameter apertures, these begin to behave like nozzles, with reduced loss of sound energy because a significant fraction of the flow does not dissipate its energy with the ISA.

The findings, although derived from controlled laboratory tests on a single wall typology, challenge the assumption that more openings, and thus more air permeability, always reduce sound insulation. The generalizability of the findings to other construction systems or field conditions should be made with caution, but nevertheless, they provide a conceptual framework for practice and serve as a basis for future studies across a broader range of building materials and in-situ conditions.

From a retrofit perspective and a practical standpoint, the data support a clear rule: prioritize sealing larger, concentrated leaks first, as they are acoustically more detrimental than many micro-openings of the same total area, especially when acoustic performance is the driving criterion. This distinction suggests a practical hierarchy for retrofit interventions.

Additionally, research findings have demonstrated that the different opening positions, based on various patterns, have no substantial impact on sound insulation for the relatively small openings under study.

In summary, the relation between air infiltration and sound insulation has been found to depend not only on the diameter and number of openings but also on the magnitude of the contact area between the air and the interior duct surface, as well as the flow

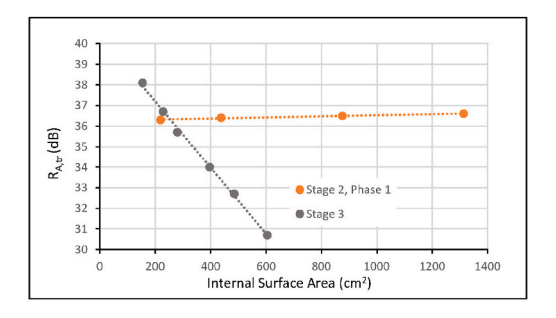


Fig. 10a. Evolution of $R_{A,tr}$ as a function of ISA.

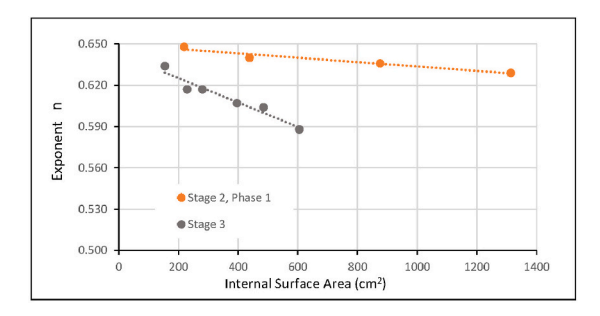


Fig. 10b. Evolution of *n* as a function of ISA.

regime adopted by the air in the infiltration path. Overall, the findings underscore the complex relationship between sound transmission and air leakage, with the flow regime playing a pivotal role in sound transmission loss. These results highlight the importance of considering opening size, patterns and flow regimes when investigating the interplay between airtightness and sound transmission in buildings.

CRediT authorship contribution statement

A. Elsaei: Writing – review & editing, Writing – original draft, Visualization, Methodology, Investigation, Conceptualization. M. Machimbarrena: Writing – review & editing, Writing – original draft, Supervision, Project administration, Methodology, Investigation, Funding acquisition, Conceptualization. A. Meiss: Writing – review & editing, Writing – original draft, Supervision, Project administration, Methodology, Investigation, Funding acquisition, Conceptualization, Data curation, Formal analysis, Validation, Visualization. I. Poza-Casado: Writing – review & editing, Supervision, Methodology. M.A. Padilla-Marcos: Methodology.

Declaration of competing interest

The authors declare that they have no known competing financial interests or personal relationships that could have appeared to influence the work reported in this paper.

Acknowledgments

This project has received funding from the European Union's Horizon Europe research & innovation programme under the HORIZON-MSCA-2021-DN-01 grant agreement No. 101072598 – "ActaReBuild".

Data availability

Data will be made available on request.

References

- [1] G. Benedetto, E. Brosio, A relation between transmission loss and air infiltration characteristics in windows, Istituto Elettrotecnico Nazionale Galileo Ferraris, Turin (1981). https://www.aivc.org/resource/relation-between-transmission-loss-and-air-infiltration-characteristics-windows.
- [2] T. Catalina, V. Iordache, F. Iordache, Correlation between air and sound propagation to determine air permeability of buildings for single/double wood pane windows, Energy Build. 224 (2020) 110253, https://doi.org/10.1016/j.enbuild.2020.110253.
- [3] D.E. Esdorn, Development of an acoustic method for the determination of the air leakage of building elements installed in a building, Kurzber. Bauforsch 19 (7) (1978) 521–527. https://www.aivc.org/resource/development-acoustic-method-determination-air-leakage-building-elements-installed-building.
- [4] V. Iordache, T. Catalina, Acoustic approach for building air permeability estimation, Build. Environ. 57 (2012) 18–27, https://doi.org/10.1016/j.
- [5] H.J. Sabine, M.B. Lacher, D.R. Flynn, T.L. Quindry, Acoustical and thermal performance of exterior residential walls, doors and windows, Natl Bur Stand Build Sci Ser 77 (1975). https://www.aivc.org/resource/acoustical-and-thermal-performance-exterior-residential-walls-doors-and-windows.
- [6] M.H. Sherman, M.P. Modera, Signal attenuation due to cavity leakage, J. Acoust. Soc. Am. 84 (6) (1988) 2163–2169, https://doi.org/10.1121/1.397062.
- [7] B. Schiricke, M. Diel, B. Kölsch, Field testing of an Acoustic method for locating air leakages in building envelopes, Buildings 2024 (4) (2024) 1159, https://doi.org/10.3390/BUILDINGS14041159.
- [8] M. Diel, B. Schiricke, J. Pernpeintner, Test facility for building envelope leakage type analysis and improvement of acoustic and thermographic airtightness measurement methods. Proceedings of 44th AIVC-12th Tightvent & 10th Venticool Conference, 2024. https://www.aivc.org/resource/test-facility-building-envelope-leakage-type-analysis-and-improvement-acoustic-and.
- [9] R.W. Graham, Infrasonic Impedance Measurement of Buildings for Air Leakage Determination, Syracuse University, 1977. https://www.aivc.org/resource/l-infrasonic-impedance-measurement-buildings-air-leakage-determination.
- [10] D.N. Keast, H.-S. Pei, The use of sound to locate infiltration openings in buildings. ASHRAE/DOE Conference "Thermal Performance of the Exterior Envelopes of Buildings, 1979. https://www.aivc.org/resource/use-sound-locate-infiltration-openings-buildings.
- [11] B. Kölsch, B. Schiricke, E. Lüpfert, B. Hoffschmidt, Detection of air leakage in building envelopes using microphone arrays. 41st AIVC/ASHRAE IAQ- 9th Tightvent 7th Venticool Conference, 2023. https://www.aivc.org/resource/detection-air-leakage-building-envelopes-using-microphone-arrays.

- [12] B. Schiricke, B. Kölsch, Acoustic method for measurement of airtightness: field testing on three different existing office buildings in Germany, 43rd AIVC -11th TightVent & 9th Venticool Conference. Ventilation, IEQ and Health in Sustainable Buildings (2023). https://www.aivc.org/resource/acoustic-method-measurement-airtightness-field-testing-three-different-existing-office.
- [13] M. Sherman, M. Modera, Low-frequency measurement of leakage in enclosures, Rev. Sci. Instrum. 57 (7) (1986) 1427–1430, https://doi.org/10.1063/
- [14] T. Sonoda, F. Peterson, A sonic method for building air-leakage measurements, Appl. Energy 22 (3) (1986) 205–224, https://doi.org/10.1016/0306-2619(86) 90003-6.
- [15] M.C. Gomperts, The "sound insulation" of circular and slit-shaped apertures, Acta Acustica united Acustica 14 (1) (1964) 1–16. https://cir.nii.ac.jp/crid/ 1570854174683602944.
- [16] M.C. Gomperts, T. Kihlman, The sound transmission loss of circular and slit-shaped apertures in walls, Acta Acustica united Acustica 18 (3) (1967) 144–150. https://cir.nii.ac.jp/crid/1574231876117830784.
- [17] B. Kölsch, B. Schiricke, J. Estevam Schmiedt, B. Hoffschmidt, Estimation of air leakage sizes in building envelope using high-frequency acoustic impulse response technique. AIVC Conference Proceedings 2019, 2019, October. https://elib.dlr.de/129823/.
- [18] J. Nurzyński, The acoustic performance of circular openings and wall-mounted vents, Appl. Acoust. 162 (2020) 107200, https://doi.org/10.1016/j.
- [19] D.J. Oldham, X. Zhao, S. Sharples, H.S. Kula, The use of acoustic intensimetry to size air leakage cracks. 12th AIVC Conference "Air Movement and Ventilation Control Within Buildings, 1991. https://www.aivc.org/resource/use-acoustic-intensimetry-size-air-leakage-cracks-0.
- [20] M. Ringger, P. Hartmann, Evaluation of an acoustical method for detecting air leaks, Air Infiltration Review 11 (1) (1989). https://www.aivc.org/resource/use-acoustic-intensimetry-size-air-leakage-cracks-0.
- [21] K. Varshney, J.E. Rosa, I. Shapiro, D. Scott, Air-infiltration measurements in buildings using sound transmission loss through small apertures, Int. J. Green Energy 10 (5) (2013) 482–493, https://doi.org/10.1080/15435075.2012.675603.
- [22] B. Kölsch, I.S. Walker, B. Schiricke, W.W. Delp, B. Hoffschmidt, Quantification of air leakage paths: a comparison of airflow and acoustic measurements, Int. J. Vent. 22 (2) (2021) 101–121, https://doi.org/10.1080/14733315.2021.1966576.
- [23] ISO 10140-2:2021 Acoustics laboratory measurement of sound insulation of building elements part 2: measurement of airborne sound insulation. https://www.iso.org/standard/79487.html, 2021.
- [24] ISO, 717-1: 2020 Acoustics—Rating of Sound Insulation in Buildings and of Building Elements—Part 1: Airborne Sound Insulation, ISO, 2020. Geneve, Switzerland, https://www.iso.org/standard/51968.html.
- [25] ISO 12999-1:2020 Acoustics determination and application of measurement uncertainties, in: Building Acoustics Part 1: Sound Insulation, second ed., 2020. Issue ISO 12999-1:2020), https://www.iso.org/standard/73930.html#lifecycle.
- [26] ISO 9972. Thermal performance of buildings. Determination of air permeability of buildings. Fan pressurization method, ISO 9972:2015), https://www.iso.org/standard/55718.html, 2015.
- [27] V. Echarri-Iribarren, R. Gómez-Val, I. Ugalde-Blázquez, Energy losses or savings due to air infiltration and envelope sealing costs in the passivhaus standard, a review on the mediterranean coast (2024), https://doi.org/10.3390/buildings14072158.
- [28] M. Sherman, A power-law formulation of laminar flow in short pipes, J. Fluid Eng. (1992), https://doi.org/10.1115/1.2910073.
- [29] C. Allen, Leakage distribution in buildings, Building Ventilation: Research and Practice (1985). https://www.osti.gov/etdeweb/biblio/5704008.
- [30] M.H. Sherman, Rengie Chan, Building Airtightness: Research and Practice (2004). https://www.aivc.org/sites/default/files/members_area/medias/pdf/Inive/LBL/LBNL-53356.pdf.